

Interpretation of "optical time-of-flight" measurements in Si

M. A. Tamor

Research Staff, Ford Motor Company, Dearborn, Michigan 48121-2053

J. P. Wolfe

*Physics Department and Materials Research Laboratory,
University of Illinois at Urbana-Champaign, Urbana, Illinois 61801*

(Received 14 August 1987)

The optical time-of-flight (TOF) technique developed by Forchel, Hillmer, and co-workers for investigation of carrier transport in Si is examined. The TOF method detects the arrival of electron-hole pairs at the surface of a thin slab following their creation by pulsed laser excitation of the opposite surface. At high excitation levels, the optical TOF data were interpreted as evidence for rapid *drift* motion of electron-hole plasma at several times the sound velocity. At low excitation levels, the optical TOF results have been interpreted in terms of diffusive transport of excitons, surface recombination, and in some analyses, macroscopic drift. We show that both the high- and low-excitation cases are consistent with a very simple model that includes only classical diffusion and surface recombination. In particular, supersonic plasma drift is not required to explain the optical TOF results.

I. INTRODUCTION

Interest in the kinetics and thermodynamics of non-equilibrium carriers in silicon has been keen for decades. This stems both from the technological importance of Si and the slightly more academic interest in the low-temperature "excitonic phases": free excitons (FE's), electron-hole droplets (EHD's), and the intermediate electron-hole plasma (EHP).¹ Luminescence spectroscopy with temporal and spatial resolution has been used extensively in studies of the phase diagram²⁻⁴ and transport properties in this system.^{5,6} The mobilities of free excitons and electron-hole droplets were measured directly using a strain gradient technique.^{5,6} In that work, a "sound-barrier" effect was observed for EHD; droplets could not be pushed to velocities higher than 5.2×10^5 cm/s on a 10-ns time scale. The increased momentum damping at near-sonic velocities originates from the degenerate Fermi-liquid nature of the electron-hole liquid (EHL) and possibly the accompanying dilation of the lattice in the liquid region.

In silicon, constant-density electron-hole droplets are formed below a critical temperature, $T_c = 24.5$ K.⁴ Spectroscopic studies have shown that when intense 10-ns excitation pulses are used above this temperature, an electron-hole plasma is formed which has a luminescence line shape noticeably broadened relative to that of an equilibrium plasma at the same temperature. To explain this anomalous broadening, Forchel *et al.*⁷ postulated that the plasma was undergoing "rapid drift" motion at velocities near the Fermi velocity (10^6 – 10^7 cm/s). Subsequent time-resolved luminescence imaging measurements by Steranka and Wolfe,⁸ determined that the electron-hole plasma created with similar 10-ns pulses actually expands at *subsonic* velocities. They also showed that the anomalous broadening could be attributed to local heat-

ing of the lattice and plasma near the excitation region.

An optical time-of-flight (TOF) method was subsequently introduced by Forchel and co-workers⁹⁻¹³ to examine the plasma transport on the nanosecond time scale. This technique employs bound-exciton luminescence from impurities implanted near one surface of a thin crystal to detect the presence of nonequilibrium carriers which were optically injected at the opposite face. With the assumption that the detected carriers traversed the sample in the form of electron-hole plasma, those authors concluded that a highly *supersonic plasma drift* occurred following the 150–300-ps laser pulse.^{9,10} More recently, transport of electron-hole plasma in Si on a sub-nanosecond time scale has been examined by Tsen¹⁴ using time-resolved Raman techniques. With 10-ps time resolution and 10- μ m spatial resolution, he found that the high-density EHP ($n \approx 3 \times 10^{18}$ cm⁻³) expanded at subsonic velocities ($\approx 2 \times 10^5$ cm/s at 35 K) parallel to the sample surface. It is important to reconcile these widely differing conclusions concerning the nature of EHP transport.

In the optical time-of-flight method a high density of In or Tl is ion implanted to a depth of roughly 2 μ m in one face of a Si slab 30–300 μ m thick.⁹⁻¹³ Carriers are optically generated by a 150–300-ps light pulse impinging on one face of the slab. Following the excitation, time-resolved luminescence from the decay of excitons bound to the implanted impurities is used as the measure of the carrier density close to the implanted surface. The $t = 0$ reference time and the time resolution of the system are established by photoexciting the implanted surface directly. When the opposite surface is excited, the time dependence of the bound-exciton luminescence may be used as a measure of carrier transport through the thickness of the slab.¹⁵ The TOF method does not distinguish the phase of the nonequilibrium carriers (FE, EHD, or

EHP) propagating through the crystal.

In the studies of EHP and EHD transport performed with a high excitation density,^{9,10} the *onset* of the impurity luminescence following excitation of the unimplanted surface was used to determine a transit time t^* . The carrier velocity, and by inference the plasma or droplet velocity, was taken to be $v^* = L/t^*$, where L is the sample thickness. At 1.8 K velocities as high as 2.0×10^6 cm/s were observed. The temperature and sample thickness dependence of v^* were modeled as a supersonic plasma expansion followed by subsonic plasma or droplet motion. It should be noted, however, that only a small fraction (<5%) of the total luminescence signal corresponded to carrier transport at supersonic velocities.

In later studies of exciton transport, the excitation was kept sufficiently weak that EHD and EHP were not formed.¹¹⁻¹³ The free-exciton mobility was obtained by fitting a diffusion equation to the time dependence of the luminescence intensity. In order to obtain good fits, Laurich and co-workers proposed a "hydrodynamic" model in which a "drift velocity" was superposed on the exciton diffusion.¹¹ The origin of this apparent drift velocity was not explained at the time.¹⁶ Subsequent studies indicated that the additional drift term may not be necessary if recombination at the sample surfaces is properly accounted for.¹² For the case of stationary (cw) excitation, Kuhn and Mahler used a quasiequilibrium Boltzmann transport equation (BTE) including thermodiffusion to demonstrate the importance of surface recombination in determining the distribution of photoexcited carriers.¹⁷ A time-dependent BTE was directly compared to TOF data in Ref. 12. In that work a BTE with infinite surface recombination at the implanted surface and variable probability for surface recombination at the excited surface was considered. The latter is equivalent to a variable surface recombination velocity. In a later paper, Mahler *et al.*¹³ indicated that the low-excitation optical TOF data are consistent with a diffusion equation (no drift motion) with recombination included. The high-excitation case was not treated.

In the present paper, we seek to unify the interpretation of low- and high-excitation transport measurements. We show that for the limit of rapid surface recombination (which seems to apply to the TOF experiments), a simple analytical model with only one adjustable parameter (the diffusion coefficient D) describes the low-excitation data very well. Furthermore, we show that the luminescence onset times observed in the high-excitation case are also consistent with diffusion and rapid surface recombination without any additional drift term. With these observations, we conclude that the wide variety of experiments on electron-hole transport in Si are in basic agreement.

II. DIFFUSION MODEL

To quantify the diffusion model a simplified diffusion equation is fit to the data presented in Ref. 11. Because the exciton bulk recombination lifetime is so much longer than the experimental time scale, particle loss is assumed to occur only at the surfaces of the sample. Thus the

equation we use is

$$\frac{\partial n(x,t)}{\partial t} = D \frac{\partial^2 n(x,t)}{\partial x^2}, \quad (1a)$$

with

$$D \frac{\partial n(x,t)}{\partial x} = sn \quad \text{at } x = 0, L, \quad (1b)$$

where D is the diffusion constant and s is a surface recombination velocity used at both surfaces (with appropriate sign). Equation (1a) does not contain the additional drift term introduced in Refs. 11 and 12. The initial carrier distribution is taken to be a δ function at the front surface, and the luminescence intensity is assumed to be proportional $n(L,t)$. We have used Eqs. (1a) and (1b) to examine both the high- and low-excitation cases. As we will show, it reproduces the temperature and sample-thickness dependence of the onset velocity v^* at high excitation, while at low excitation the entire time dependence of the bound-exciton luminescence is reproduced.

Equations (1a) and (1b) are solved by two different methods. The first is a finite-differences method which generates the time dependence of the carrier density near the implanted surface. The boundary conditions can be adjusted to include surface recombination at either or both surfaces. For purposes of comparison, a drift velocity may also be included. The second solution uses the method of images to obtain an analytic solution in series form for the limiting cases where s at either surface is either zero or infinite. Where the boundary conditions forced $n(L,t) = 0$ (infinite s at the implanted surface), the exciton density is evaluated infinitesimally inside the sample. For purposes of comparison, the time dependences were normalized to the peak value. Once normalized, transients with recombination at the front (excited) surface only were indistinguishable from those with recombination at the back (implanted) only. In the series solution the similarity of the time dependences for the two cases is also found analytically. Because only the first term in the series is significant at early times, the rising side of the luminescence transient is accurately described by the analytic form:

$$n(L,t) \propto (t)^{-3/2} e^{-L^2/4Dt}, \quad (2a)$$

$$n(L,t) \propto (t)^{-5/2} e^{-L^2/4Dt}, \quad (2b)$$

where Eq. (2a) applies where surface recombination occurs at either surface and (2b) applies where recombination occurs at both surfaces.

III. RESULTS

Figure 1 shows transients calculated using the finite-differences method for $D = 200$ cm²/s in a 100- μ m-thick slab. The figure shows the effect of including recombination at only one surface, both surfaces, and substitution of a drift velocity for recombination at one surface by adding $-v_d(\partial n/\partial x)$ to the right-hand side of Eq. (1a). (The values of D , s , and v_d were chosen for direct comparison to Fig. 6 of Ref. 11.) The transient for $s = 1 \times 10^5$

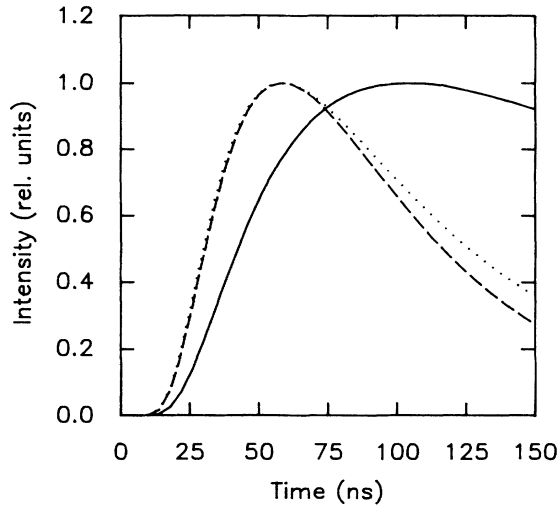


FIG. 1. Calculated luminescence transients for a 100- μm -thick specimen and $D=200\text{ cm}^2/\text{s}$. The solid curve is for recombination at only one surface with $s=10^5\text{ cm/s}$. The dashed curve is for the same boundary conditions, but with a drift velocity, $v_d=2\times 10^5\text{ cm/s}$, superposed. The dotted curve is for zero drift velocity, but with recombination at both surfaces with $s=2\times 10^5\text{ cm/s}$.

cm/s at one surface and $v_d=2\times 10^5\text{ cm/s}$ is very similar to that for $v_d=0$ and $s=2\times 10^5\text{ cm/s}$ at both surfaces. This demonstrates that omission of recombination at either surface may be "compensated" by the introduction of the (artificial) drift velocity. The stated necessity of the drift velocity in Refs. 11 and 12 suggests that the diffusion model used by those authors included recombination at only one surface.

Having eliminated the "drift" velocity as a necessary parameter, we now consider the significance of the finite

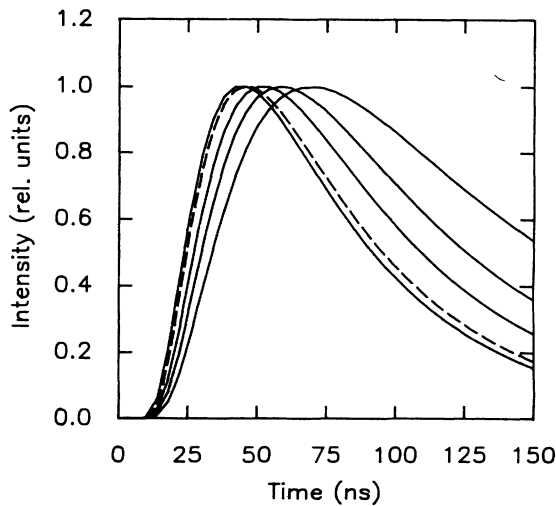


FIG. 2. Series of calculated transients for a 100- μm -thick specimen with $D=200\text{ cm}^2/\text{s}$, zero drift velocity, and increasing s at both surfaces. From top to bottom at the right-hand border, $s=1\times 10^5\text{ cm/s}$, $2\times 10^5\text{ cm/s}$, $4\times 10^5\text{ cm/s}$, and $s=\infty$. The dashed curve is the analytic result for infinite s . The small discrepancy is due to accumulated error in the finite-differences method.

surface recombination velocity. Figure 2 shows a series of calculated transients for a 100- μm -thick slab and $D=200\text{ cm}^2/\text{s}$ with increasing recombination velocity at both surfaces. The limiting analytic result (the dashed line, $s=\infty$ at both surfaces) is also shown to indicate the agreement between the two solutions. The transients appear to scale in time with no major change in shape.

To test how accurately the "infinite- s " case reproduces the transients with finite s , the analytic form was "fit" to the results in Fig. 1. Figure 3 shows that using $D=160\text{ cm}^2/\text{s}$ and infinite s at both surfaces produces a transient nearly identical to that for $D=200\text{ cm}^2/\text{s}$ and $s=2\times 10^5\text{ cm/s}$ at both surfaces. The figure also shows a transient calculated using $D=260\text{ cm}^2/\text{s}$ and $s=10^5\text{ cm/s}$ at both surfaces. For the purposes of comparison with noisy experimental data, these three transients are virtually indistinguishable. Thus the TOF method is not a very accurate method of determining D and s from a two-parameter fit.

Figure 4 shows results of a similar test for a thinner sample (28 μm versus 100 μm). Although the effect of the finite s is somewhat greater for the thinner specimens, in neither case does a recombination velocity greater than about $2\times 10^5\text{ cm/s}$ produce a transient significantly different than that for infinite s . In other words, for $s\gtrsim 2\times 10^5\text{ cm/s}$, a range of combinations of D and s produce nearly equivalent transients. Therefore, for simplicity and consistency, we analyze the experimental results using the simplified model which assumes infinite surface recombination velocity at both surfaces. D is the only free parameter.

A. Low excitation

We consider first the low-excitation case. The symbols in Figs. 5 and 6 show the results of the fits to the data published as Figs. 7(a) and 7(b) of Ref. 11. At both 1.8

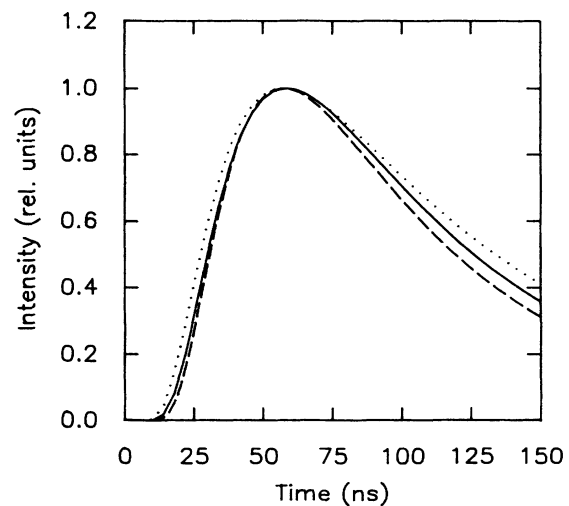


FIG. 3. Calculated luminescence transients for a 100- μm -thick specimen showing the interaction between D and s . The solid curve was calculated using the same parameters as in Ref. 11: $D=200\text{ cm}^2/\text{s}$ and $s=2\times 10^5\text{ cm/s}$. The dashed curve is for $D=160\text{ cm}^2/\text{s}$ and $s=\infty$. The dotted curve is for $D=260\text{ cm}^2/\text{s}$ and $s=10^5\text{ cm/s}$. The values of D and s were chosen so that the transients all peak at the same time.

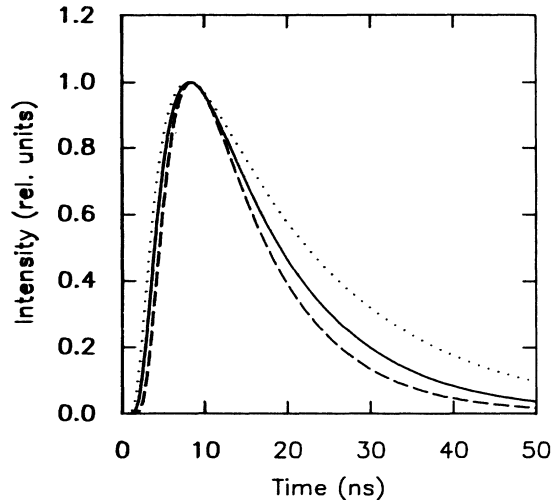


FIG. 4. Calculated transients for a 28- μm -thick specimen. The solid curve indicates $D = 140 \text{ cm}^2/\text{s}$ and $s = 2 \times 10^5 \text{ cm/s}$. The dashed curve is for $D = 93 \text{ cm}^2/\text{s}$ and $s = \infty$. The dotted curve is for $D = 200 \text{ cm}^2/\text{s}$ and $s = 10^5 \text{ cm/s}$.

and 10 K the data and the earlier fit (continuous lines in the figures) using a drift velocity and finite surface recombination velocity are reproduced. The new values of the diffusion coefficient are about two-thirds of the values obtained by Laurich *et al.*¹¹ The magnitude and temperature dependence of C can be parametrized as $D = 210/T^{1/2} \text{ cm}^2/\text{s}$. This is in rough agreement with the measurements of exciton mobility obtained directly by the strain gradient method. Using the measured mo-

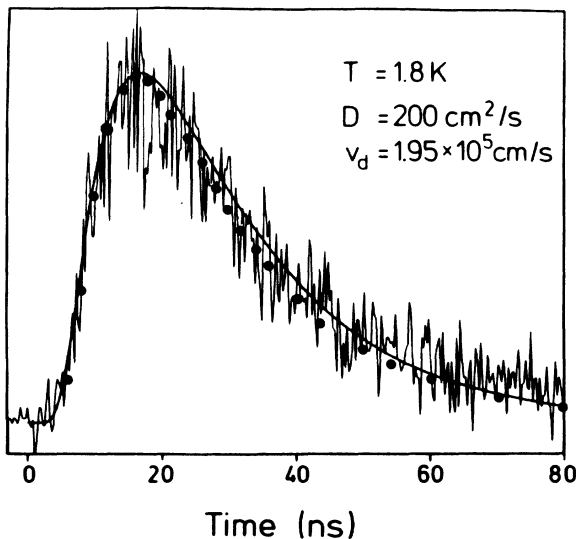


FIG. 5. Time dependence of the impurity-bound exciton luminescence following pulsed optical excitation of the unimplanted surface of a 53- μm -thick Si slab at 1.8 K. The symbols show the transient produced by Eqs. (1) with $D = 145 \text{ cm}^2/\text{s}$ and infinite surface recombination velocity, at both surfaces. Figures 5 and 6 are reproduced exactly from Ref. 11. The solid lines represent those authors' fit to the data using $s = 1 \times 10^5 \text{ cm/s}$ at one surface and the parameters as displayed in the figures.

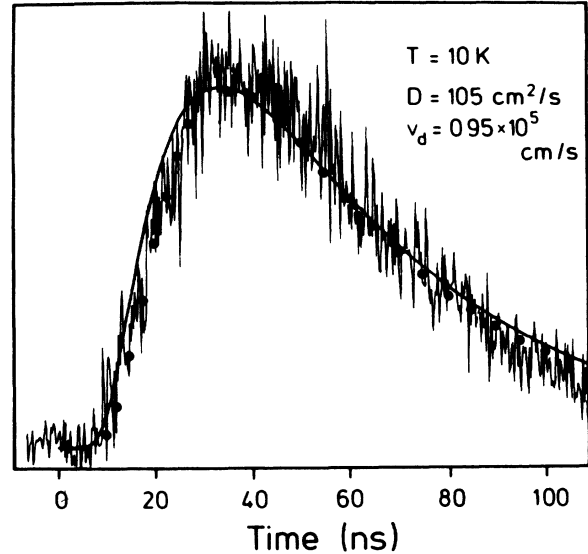


FIG. 6. Time dependence of the bound-exciton luminescence from a 53- μm -thick sample at 10 K. The symbols indicate the dependence from Eqs. (1) using $D = 65 \text{ cm}^2/\text{s}$ and infinite s .

bility $\mu = 3.5 \times 10^6 / T^{3/2} \text{ cm}^2 \text{ s}^{-1} \text{ V}^{-1}$ and the Einstein relation $D = \mu kT$, we obtain $D = 310/T^{1/2}$.⁵ This is also in agreement with the values obtained from time-resolved luminescence imaging of the spatial expansion of the exciton cloud driven deep into the sample by pulsed excitation.⁸

As a further test of the simplified model, the data from Ref. 12 for a thin (28- μm -thick) sample were "fitted" by determining the time at which the luminescence decayed the one-half its peak intensity and finding the value of D that reproduced that "half-time." The values of D so obtained were again about two-thirds the values obtained using s as a fit parameter. The values of D for the thin samples were consistently about one half those obtained for the thicker specimens at the same temperatures. This discrepancy also appears in the previous authors' own analysis which retains s as a parameter.¹² These results indicate a thickness dependence of D that is not understood at present but may be due to deep damage to the polished sample surfaces. This hypothesis is consistent with the very large (essentially infinite) recombination velocity. Due to the ambiguity in the choice of surface recombination velocity and the apparent dependence of D on sample thickness, the optical TOF method cannot presently be used for an accurate determination of the diffusion coefficient. However, given an independent determination of D , the optical TOF method could provide a quantitative measurement of s .

B. High excitation

Next we extend the all-diffusion (no drift) model to the high-excitation case. As noted above, in those studies a velocity was determined from an "onset" time t^* and the sample thickness L . We define t^* in terms of the times at which the signal $n(L, t)$ reached 10% and 90% of its ultimate maximum value. The extrapolation through these

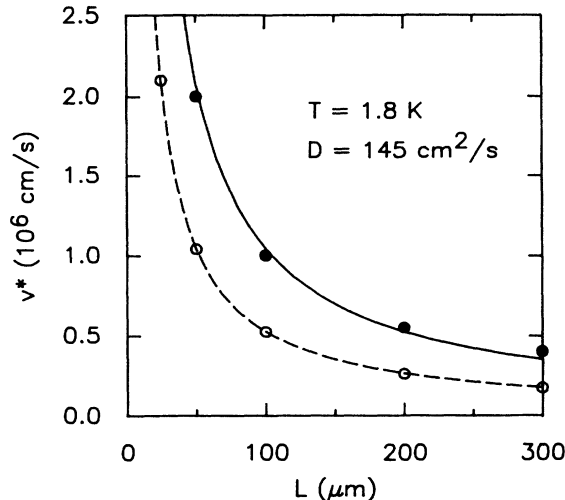


FIG. 7. Sample thickness dependence of v^* at 1.8 K using $D = 145 \text{ cm}^2/\text{s}$. The open symbols are determined from the onset time defined in the text. The dashed curve is the parametric dependence $v^* = 36D/L$. The solid symbols are reproduced from Ref. 9, while the solid curve represents the adjusted parametric fit $v^* = 70D/L$.

two points back to the zero signal baseline determines t^* . The open symbols in Fig. 7 shows $v^* = L/t^*$ for several sample thicknesses with $D = 145 \text{ cm}^2/\text{s}$ and infinite s at both surfaces. The dependence can be very accurately parametrized as $v^* = 36D/L$ (the dashed curve in the figure). [Equation (2b), which is accurate at early times, also shows $v^* = 36D/L$.] The solid symbols in Fig. 7 are TOF results for Ref. 9. The solid curve indicates the same parametrization using an adjusted scale factor, $v^* = 70D/L$, and fits the experimental results well. The scale factor will depend on the experimental definition of the onset time. Alternatively, the value of D in the high-excitation case may be larger than that of free excitons.

The measured temperature dependence of v^* for a 100- μm thick specimen is shown in Fig. 8 (also from Ref. 9). The solid line in the figure is a parametrization similar to that just described using the measured temperature dependence of the diffusion coefficient $D = 210/T^{1/2}$. The scale factor was the same as that used for the solid curve in Fig. 7. Thus, the solid curve in Fig. 8 represents $v^* = (70 \times 210)/LT^{1/2}$ which is also in good agreement with the measurements. Figures 7 and 8 show that the observed temperature and sample thickness dependences of the luminescence onset time is satisfactorily explained by *diffusion* of light particles—excitons or electron-hole pairs. Rapid drift of the high density electron-hole plasma or droplets is not required to explain the TOF results.

While the diffusion model has reproduced the onset of the luminescence, the effects of EHD's and EHP at later time has not been considered. The EHD's and EHP will be pushed by phonon wind forces.⁸ However, phonon wind cannot induce supersonic motion. Although Hillmer *et al.* (Ref. 13) have shown that the presence of EHD's does not directly affect the bound exciton luminescence, EHD's do evaporate and so are a long-lived source of free carriers or excitons which will greatly

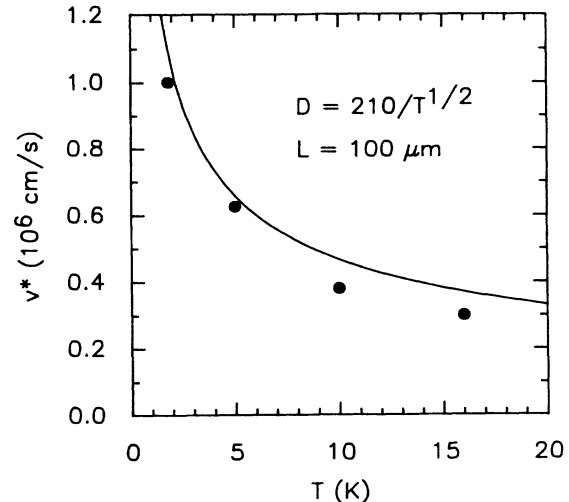


FIG. 8. Temperature dependence of v^* for a fixed sample thickness of 100 μm . The symbols are data from Ref. 9. The solid curve is the result of combining the temperature dependence of D , $D = 210/T^{1/2}$, with the adjusted parametrization from Fig. 7, $v^* = 70D/L$, to obtain $v^* = 1.5 \times 10^4 / (LT^{1/2})$.

extend the luminescence transient. This is exactly what was observed: At low temperature and high excitation the luminescence peaked at progressively later times as the excitation was increased, while the onset time remained unchanged.^{9,10} The effect of EHP is probably more complicated. The plasma expansion may be driven both by diffusion and phonon wind forces. The diffusion coefficient for the plasma should be density dependent and may differ somewhat from that of free excitons. If conditions are favorable for the plasma to form a constant-density phase, as observed by Smith and Wolfe,⁴ its effect may be similar to that of EHD's.

IV. CONCLUSIONS

We have shown that the optical TOF data can be accurately reproduced by a very simple model including only diffusion and surface recombination at *both* sample faces. Our analysis of the high-excitation data does not support the contention that the high-density EHD's or EHP undergo supersonic drift on these distances (20–300 μm) and time scales (1–100 ns). In the TOF data, the luminescence due to carriers arriving with supersonic velocities contributes only a small fraction ($< 5\%$) to the time-integrated signal. We believe that it is not realistic to identify the small number of rapidly diffusing particles that determine the onset time t^* in the TOF measurement with the dense electron-hole plasma that dominates the photoluminescence spectrum.⁸ In effect, it is not the high-density phase, EHP or EHD, which traverses the sample with supersonic velocity. Therefore, the optical TOF results do not contradict the sound barrier for electron-hole droplets⁶ and the subsonic plasma expansion⁷ observed by direct-photoluminescence imaging and spectral analysis. We conclude that the time-resolved photoluminescence spectra, time-resolved imaging

and optical TOF results contain no essential contradictions. Indeed, together they provide a rather complete

picture of plasma and exciton transport in silicon on the nanosecond and longer time scale.

-
- ¹J. C. Hensel, G. A. Thomas, T. G. Phillips, and T. M. Rice, in *Solid State Physics*, edited by H. Ehrenreich, F. Seitz, and D. Turnbull (Academic, New York, 1978), Vol. 32.
- ²P. L. Gourley and J. P. Wolfe, *Phys. Rev. B* **25**, 1125 (1982).
- ³L. J. Schowalter, F. M. Steranka, M. B. Salamon, and J. P. Wolfe, *Phys. Rev. B* **29**, 2970 (1984).
- ⁴L. M. Smith and J. P. Wolfe, *Phys. Rev. Lett.* **57**, 2314 (1986).
- ⁵M. A. Tamor and J. P. Wolfe, *Phys. Rev. Lett.* **44**, 1703 (1980).
- ⁶M. A. Tamor and J. P. Wolfe, *Phys. Rev. B* **26**, 5743 (1982).
- ⁷A. Forchel, H. Schweizer, and G. Mahler, *Phys. Rev. Lett.* **51**, 501 (1983).
- ⁸F. M. Steranka and J. P. Wolfe, *Phys. Rev. Lett.* **53**, 2181 (1984); *Phys. Rev. B* **34**, 1014 (1986).
- ⁹A. Forchel, B. Laurich, H. Hillmer, G. Trankle, and M. Pilkuhn, *J. Lumin.* **30**, 67 (1985).
- ¹⁰A. Forchel, B. Laurich, G. Trankle, G. Mahler, T. X. Hoai, and A. Axman, *Proceedings of the 17th International Conference on the Physics of Semiconductors, San Francisco, 1984*, edited by J. D. Chadi and W. A. Harrison (Springer-Verlag, New York, 1985), p. 1285.
- ¹¹B. Laurich, H. Hillmer, and A. Forchel, *J. Appl. Phys.* **61**, 1480 (1987).
- ¹²H. Hillmer, T. Kuhn, B. Laurich, A. Forchel, and G. Mahler, *Phys. Scr.* **35**, 520 (1987).
- ¹³G. Mahler, T. Kuhn, A. Forchel, and H. Hillmer, *Optical Nonlinearities and Instabilities in Semiconductors, 1986*, edited by H. Haug (Academic, New York, 1987).
- ¹⁴K. T. Tsen, *Phys. Rev. B* **35**, 4134 (1987).
- ¹⁵The optical TOF method is very similar to the method used by Zinov'ev *et al.* to measure the diffusion to excitons in CdS. N. N. Zinov'ev, L. P. Ivanov, I. G. Lang, S. T. Pavlov, A. V. Prokaznikov, and I. D. Yaroshetskii, *Pis'ma Zh. Eksp. Teor. Fiz.* **36**, 12 (1982) [*JETP Lett.* **36**, 15 (1982)].
- ¹⁶References 11, 12, and 13 are not consistent in their analysis of the TOF data. In Ref. 11 finite surface recombination (with s fixed) and a "drift" velocity were assumed. In Ref. 12 it appears that infinite s was assumed but v_d was retained. This is inferred from the reference to the use of the method of images which may be used for a time-dependent solution only for zero or infinite s at a given surface. As noted in the text, the necessity of v_d in obtaining good fits is an indication that recombination was included at only one surface. In Ref. 13, v_d was dropped from the fitting procedure, but a temperature-dependent recombination velocity at both surfaces was assumed.
- ¹⁷T. Kuhn and G. Mahler, *Phys. Rev. B* **35**, 2827 (1987).